
Compressibility: Power of PCA in Clustering Problems Beyond Dimensionality Reduction

Chandra Sekhar Mukherjee *
Department of Computer Science
University of Southern California
chandrasedkhar.mukherjee07@gmail.com

Jiapeng Zhang †
Department of Computer Science
University of Southern California
jiapengz@usc.edu

Abstract

In this paper we take a step towards understanding the impact of principle component analysis (PCA) in the context of unsupervised clustering beyond a dimensionality reduction tool. We explore another property of PCA in vector clustering problems, which we call compressibility. This phenomenon shows that PCA significantly reduces the distance of data points belonging to the same clusters, while reducing inter-cluster distances relatively mildly. This gap explains many empirical observations found in practice. For example, in single-cell RNA-sequencing analysis, which is an application of vector clustering in biology, it has been observed that applying PCA on datasets significantly improves the accuracy of classical clustering algorithms such as K-means.

We study this compression gap in both theory and practice. On the theoretical side, we analyze PCA in a fairly general probabilistic setup, which we call the random vector model. In terms of practice, we verify the compressibility of PCA on multiple single-cell RNA-seq datasets.

1 Introduction

Principal component analysis (PCA) is one of the most fundamental tools used in machine learning. PCA has two primary applications, dimensionality reduction and noise reduction. In the former setup, PCA is used to transform high dimensional data to lower dimensions for better visualizations as well as a heuristic that reduces the complexity of the algorithms that are to be run on the data. In the second paradigm, PCA is used to remove the noise in the data using the fact that the data shows high variance along the principle components.

In this paper, we analyze PCA in vector clustering problems. In this problem, the input is a list of vectors, we hope to cluster these vectors according to their “similarities”. The vector clustering is one of the fundamental unsupervised learning problems, with a wide range of applications and heuristics. Before introducing our main results, we first quote an observation from biologists. In a comprehensive survey (KAH19), authors compared many clustering algorithms according to their observation from single-cell data. Interestingly, in a comparison of K-means and first apply PCA, and then run K-means on vectors after PCA, they made the following comments.

- K-means “*performs poorly when there are no rare cell types.*”
- PCA+K-means achieves “*high accuracy through consensus.*”

From this observation, it seems that PCA plays an important role for vector clustering problems (at least for single-cell analysis). Furthermore, many papers observed that PCA always helps to

*Research supported by NSF CAREER award 2141536.

†Research supported by NSF CAREER award 2141536.

boost the accuracy of clustering. One of the most popular single-cell clustering algorithms, Seurat (HHAN⁺21) also uses PCA on the matrix before converting it to a graph to run a graph clustering algorithm such as Louvain algorithm.

In this paper, we study the reason behind this phenomenon. Roughly speaking, we show that PCA compresses the ℓ_2 -norm distance of vectors from the same clusters. Specifically, for two points u and v if we denote by $\Pi(u)$ and $\Pi(v)$ the post-PCA projection then the ratio $\frac{\|u-v\|}{\|\Pi(u)-\Pi(v)\|}$ is much larger for intra-cluster points than for the inter-cluster case. Thus, this suggests that PCA itself is a good step towards clustering, irrespective of the algorithms that are applied on the post-PCA data. In fact, PCA itself solving the clustering problem for a large case of parameters, and strictly improving the relative distances for a larger case. Many popular algorithms (such as K-means) use the ℓ_2 -norm distance to measure the similarity, hence the compressibility is a good explanation for the observation by (KAH19). We analyze this phenomenon in two ways, focusing on the *uncentered* principle component analysis.

On the theoretical side, we study clustering in a random vector model, where the vectors (datapoints) are expressed as a mixture of underlying signal and noise, with the noise acting on each feature independently in an arbitrary fashion. Crucially, we do not make any distributional assumption on the noise such as Gaussian or Bernoulli. We show that under a fairly generic (and empirically verifiable) characterization of the signal and noise, PCA drastically improves the dataset.

On the experimental side, we verify the compressibility of (uncentered) PCA and its effect on clustering algorithm on real data sets. We mainly focus on single-cell RNA-seq data. Single-cell sequencing is one of the major breakthrough in biology in last two decades, and correct clustering of these datasets have significant impact in the development of immunology, among other fields (KAH19; VKS17). In the single-cell data, the features are genes and each datapoint (vector) is a cell, for which the expression values of the different genes are recorded. Due to the sensitive and complex nature of single-cell RNA sequencing data, it is hard to obtain large datasets with true labeling. We run our experiments on two datasets with approximately 24,000 genes and around 2500 cells, and verify that uncentered-PCA indeed performs relative compression of the data with respect to the true clusters. Furthermore, we observe that the accuracy of Louvain’s algorithm (Seurat) for this dataset can be directly connected to this compression where clusters with better compression are identified with better accuracy.

1.1 Precursors and Comparisons

The impact of PCA on single-cell RNA-sequencing clustering is well documented in literature (KAH19; VKS17). However, there is no theoretical explanation of this phenomenon that applies to any Euclidean distance based clustering algorithm. In this direction we show that uncentered PCA improves the relative distance of data in the random vector model, and we provide experiments on real datasets that support our analytical results. Our theoretical setup and experimental results are both based on the *uncentered*-PCA, where the data is not mean centered. In this regard we describe generic situations where centering does not help in relative compression. Furthermore, we provide empirical evidence that supports that centering is not a necessary step for PCA in relation to clustering of single cell RNA-sequencing data.

From a theoretical perspective, random vector clustering has been an interesting problem in learning theory. Our definition of random vector model was inspired by (and a generalization of) a closely related area called *stochastic block model* (SBM). In the SBM model, there is a graph $G(V, E)$ with n vertices and k unknown ground truth clusters. If two vertices belong to same clusters, there is an edge between them with probability p , otherwise there is an edge with probability q , where $p > q$. Then the adjacency matrix of G is a special symmetric case of \hat{A} . Given an instantiation of such a graph, the problem is to recover the clusters. There has been extensive work in the SBM. We refer (Abb18) for a comprehensive survey. In this paradigm spectral algorithms are shown to be really powerful in recovering clusters (McS01; VU18). In fact PCA can be thought of as a very simple spectral algorithm, and our theoretical analysis of PCA borrows ideas from (VU18)’s analysis for spectral algorithms for SBM.

In the more general non symmetric rectangular case, most of the work has mainly been done considering only considering two underlying clusters (CZ18), and/or the noise is assumed to be Gaus-

sian (JW16). Furthermore, *the aforementioned algorithms do not concentrate on the simple PCA procedure for clustering*, which the primary objective of our paper.

Single-cell RNA-sequencing data is of course not symmetric. Furthermore the Gaussian distributional noise assumption is not generically justifiable. In fact it has been observed that in certain cases the Beta-Poisson distribution models the data best (VWK⁺16). In comparison our analysis doesn't require the dataset to be square and we do not make any distributional assumption, aside from independence. This way we generalize both the SBM model and non-symmetric models with Gaussian noise distribution. It should be noted that obtaining tight bounds is not the primary objective of this paper. We aim to establish a sound theoretical insight behind the use of PCA in clustering algorithms, and its impact beyond a dimensionality reduction tool.

Against this backdrop, we lay out the organization of the rest of the paper.

Organization In Section 2 we describe our results including both theoretical and experimental parts. We also compare our results with that of the more commonly used centered-PCA and explain how our observations are extendable to that case as well. In Section 3 we present our theoretical result, proving the main theorem on the random vector model. Section 4 describes our experiments in more detail, explaining some of our secondary observations. In Section 5, we conclude the paper with a discussion on how our analysis may be helpful for designing better algorithms and future directions, both in theoretical and implementation direction.

2 Setup and Main Results

2.1 Random Vector Model and Relative Compression due to PCA

We now describe our random vector clustering setup. The dataset consists of n vectors $\mathbf{u}_i \in \mathbb{R}^d$, $1 \leq i \leq n$. Each vector(datapoint) belongs to one of k -underlying clusters V_1, \dots, V_k . Together, the dataset is expressed as a $d \times n$ matrix \hat{A} . The dataset is structured as follows.

1. Each cluster V_j has a unknown ground-truth center $c_j \in \mathbb{R}^d$.
2. Additionally, the cluster V_j , $1 \leq j \leq k$ is associated with a distribution $\mathcal{D}^{(j)} \in \mathbb{R}$ such that $\mathcal{D}^{(j)}$ is coordinate wise independent 0-mean arbitrary distribution.

The random vector clustering data is then set up as follows.

Definition 1 (Random Vector Clustering-Dataset). *In the dataset \hat{A} , if a vector \mathbf{u}_i belongs to cluster V_j , then it is sampled as $\mathbf{u}_i = c_j + \mathbf{e}_i$ where $\mathbf{e}_i \sim \mathcal{D}^{(j)}$.*

Remark 1. *We remark that $\mathcal{D}^{(j)}$ does not only capture the technical noise present in the dataset due to experiment, but it also captures the inherent randomness present in the data itself (e.g., gene expression of the cells are sampled from a distribution)*

That is, each vector of \hat{A} is a sum of the ground-truth cluster center and a random vector, which account for both technical noise and inherent randomness in the data. Here, the only restriction on the distributions $\mathcal{D}^{(j)}$ is that they are coordinate wise independent and have zero mean, i.e. for each coordinate $\ell \in [d]$, $\mathbb{E} [\mathcal{D}_\ell^{(j)}] = 0$. The variance of all the coordinate wise random variables in the distributions is upper bounded as

$$\max_{1 \leq j \leq k, 1 \leq \ell \leq d} \text{Var} \left(\mathcal{D}_\ell^{(j)} \right) =: \sigma^2$$

For sake of simplicity we also denote $\sigma_j^2 = \sum_{\ell=1}^d \text{Var} \left(\mathcal{D}_\ell^{(j)} \right)$. Next we formally define the uncentered PCA projection before proceeding to describe the compression property of our interest.

Definition 2 (Uncentered PCA: $P_{\hat{A}}^k$). *Given the matrix \hat{A} , $P_{\hat{A}}^k$ is the uncentered PCA projection operator, which is a $k \times d$ linear operator. It comprises of the top left k singular vectors of \hat{A} , i.e. the top k eigenvectors of $\hat{A}(\hat{A})^T$. The operation $P_{\hat{A}}^k(\mathbf{u})$ implies matrix multiplication of $P_{\hat{A}}^k$ with \mathbf{u} that results in a k -dimensional vector.*

Here s_k is the k -th singular value of \hat{A} .

With respect to this definition we have the following phenomenon.

Definition 3 (Relative Compression of PCA). *Let \mathbf{u} and \mathbf{v} be any two vectors in the data set \hat{A} and $P_{\hat{A}}^k(\mathbf{u})$ and $P_{\hat{A}}^k(\mathbf{v})$ be their projection due to the top k Principle components. We define the k -PC compression of two vectors \mathbf{u} and \mathbf{v} as the ratio*

$$\Delta_{\hat{A},k}(\mathbf{u}, \mathbf{v}) = \frac{\|\mathbf{u} - \mathbf{v}\|}{\|P_{\hat{A}}^k(\mathbf{u}) - P_{\hat{A}}^k(\mathbf{v})\|}$$

The main theoretical result of this paper is that under certain conditions, the projection due to PCA relatively compresses the distance between intra-cluster vectors(datapoints) to a much higher degree as compared to vectors belonging to different clusters. We now formally describe our result.

Theorem 1. *Let \hat{A} be a $d \times n$ dataset setup in the random vector clustering model with k ground truth clusters, so that all column vectors $\mathbf{u} \in \hat{A} \in [0, 1]^d$. Let s_k be the k -th singular value of \hat{A} . Then with probability $1 - \mathcal{O}(n^{-1})$, for some constant C_0 s.t $\sigma \geq C_0 \frac{\log n}{n}$, the k -PC compression ratio, $\Delta_{A,k}(\mathbf{u}, \mathbf{v})$ of all intra-cluster pairs of points $\mathbf{u}, \mathbf{v} \in V_j$ is lower bounded by*

$$\frac{\sqrt{2d\sigma_j^2 - 12\sqrt{d} \log n}}{2\sqrt{2} \left(\sqrt{k} \left(\sigma + \sqrt{16 \log(nk)} \right) + \frac{C_0 \sigma^2 \sqrt{d(d+n)}}{s_k} \right)} \quad (1)$$

Similarly, the compression ratio of all inter-cluster pairs, i.e., $\Delta_{A,k}(\mathbf{u}, \mathbf{v})$ is upper bounded by

$$\frac{\sqrt{d(\sigma_j^2 + \sigma_{j'}^2) + \|c_j - c_{j'}\|^2 + 12\sqrt{d} \log n}}{\sqrt{2} \left(\|c_j - c_{j'}\| - 2 \left(\sqrt{k} \left(\sigma + \sqrt{16 \log(nk)} \right) - \frac{C_0 \sigma^2 \sqrt{2(d+n)(\|c_j - c_{j'}\|^2 + d(\sigma_j^2 + \sigma_{j'}^2))}}{s_k} \right) \right)} \quad (2)$$

with probability $1 - \mathcal{O}(n^{-1})$.

In this theorem, we assume all entries of \hat{A} to be bounded within $[0, 1]$. It can be relaxed to any constant C . If we choose a larger C , the denominator will get multiplied by a factor of C .

2.1.1 Interpreting Theorem 1:

The implication of Theorem 1 is that, for many choices of parameters, the compression ratio of intra-cluster pairs is much larger than the compression ratio of inter-cluster pairs. In particular, single-cell data falls in this regime based on our observation. In single-cell data, the pre-PCA distance of intra-cluster pairs and the pre-PCA distance of inter-cluster pairs are very close, which means that the distributions $\mathcal{D}^{(j)}$ affects the pre-PCA distance significantly, causing the numerators of Equations (1) and (2) are very similar. Now we focus on the denominators. To achieve a non-trivial gap on the denominators between the intra cluster inter cluster pairs, we need the following two requirements:

1. For all $j \neq j'$, $\|c_j - c_{j'}\|$ is much larger than \sqrt{k} ;
2. The k -th singular value of \hat{A} is much larger than $\sqrt{d+n}$.

These two requirements are satisfied in many natural clustering models, including the SBM model.

Given the aforementioned example, it may seem appropriate to use just post PCA distances (instead of compression) of points as a metric of understanding PCA's impact on clustering data. However, compressibility has an advantage. The reason is that the pre and post PCA distances are affected by the different values of σ_j , the total variances for different clusters. In natural theoretical models as well as in real datasets (such as single-cell data), different σ_j values may lead to an interesting situation. We may have two clusters $V_j, V_{j'}$ with $\sigma_j > \sigma_{j'}$ so that the average post PCA "intra-cluster" distances of points in $V_{j'}$ may be similar to the average post PCA "inter-cluster" distances of points in V_j (For example, the cluster 7 and the cluster 4 in Table 2).

In such case, the compression ratio becomes a more expressive variables with average compression ratio of intra cluster pairs being higher than that of inter cluster pairs. Thus, compressibility can be thought as a more expressive, scale invariant metric of PCA's impact on clustering data, as compared to post PCA distance. We refer Section 2.2.1 for more details.

Remark 2. A natural question here is understanding the consequence of taking the top k' principle components instead of the top k in our projection, since it may not be possible to know the number of ground truth clusters.

As a high level explanation, one gets the best compression for $k' = k$. Furthermore, we show in Section 3.4 that if $k' = k + c$ for some constant c , the relative compression due to PCA is still significant, for $1 - o(1)$ -fraction of the pairs.

However, in practice PCA's compression ability seem to not be adversely affected by choosing $k' = k \pm c$, and we believe our current limit of analysis can be overcome.

Now we discuss the single-cell data in detail, and describe our experimental results.

2.2 Single-cell RNA-seq analysis

In single-cell sequencing, a large number of cells (denoted by n) are isolated and their transcriptomes are profiled through RNA sequencing. For each cell, the sequencing result is represented by a d -dimensional vector \mathbf{u} , where d is the number of genes. The ℓ -th coordinate of \mathbf{u} represents the expression value of the cell on the ℓ -th gene. This creates a d -dimensional dataset of n cells. This is the dataset of our interest, which we express as the $d \times n$ matrix \hat{A} . From hereon we refer to the vectors of \hat{A} as $\mathbf{u}_i, 1 \leq i \leq n$. According to the report by *Human Genome Project*, the number of human genes should be at least 46,831 including both coding genes and non-coding genes. For example, the first dataset that we consider has 1809-cells, and the expression values of ≈ 24000 genes are noted.

Then the clustering task is to group cells according to their type. In biology, same-type cells should have similarity in the expression of certain genes. Hence it is essentially a vector clustering problem. Against this background we verify the compressibility of PCA on single-cell data through two datasets on mouse cells. These are two of the standard single-cell RNA-seq data (KMA⁺15; TMN⁺16) with true labels, i.e., the true type of each cells.³ For these data sets we have the true labels that were obtained by the author of these datasets from biological experience. First we go through a pre-processing step called log-normalization.

Log normalization In this step we simply make the transformation $\hat{A}_{i,j} = \log(\hat{A}_{i,j} + 1)$. This is a standard step used in many single-cell clustering algorithms, including Seurat and PCA+K-means, to reduce the effect of housekeeper gene. Housekeeper genes are these genes have large expression, but all cells (even from different clusters) have similar expression. Hence it might hurt the clustering results.

Empirical Evidence Based on this dataset we define the intra-cluster average distance of a cluster C_j as $\mathbb{E}_{\mathbf{u}, \mathbf{v} \in C_j} [\|\mathbf{u} - \mathbf{v}\|]$. Similarly we have the pre-PCA inter-cluster average distance as $\mathbb{E}_{\mathbf{u} \in C_j, \mathbf{v} \notin C_j} [\|\mathbf{u} - \mathbf{v}\|]$. Similarly, the post pca distances are obtained by replacing $\|\mathbf{u} - \mathbf{v}\|$ with $\|P_{\hat{A}}^k(\mathbf{u}) - P_{\hat{A}}^k(\mathbf{v})\|$. Similarly we find the average compression ratio by taking an average of the compression of the individual pairs. We note down our outcomes in Tables 1 and 2. Our results show that the average compression ratio is consistently higher for the intra-cluster cases. This can be related to a loose version of Theorem 1, as here we look into the average compression ratio instead of the individual pairs. We provide the plot of the expected intra-cluster and inter-cluster distances for each point in Section 4.

2.2.1 Some important observations

Here we note down some of the observations on the datasets that justify some interpretations and rationales behind the framing of Theorem 1.

First, we observe that in the original dataset, the average inter-cluster distances for some cluster can be same or even less than the average intra-cluster distance for some other clusters. For example, $C1$ and $C4$ in dataset-1, and $C2$ and $C7$ in dataset-2. Intuitively, these clusters should be very hard to be identified by a K-means objective driven algorithm. However, the post PCA inter-cluster distance

³There is only a few number of dataset with true label online.

of $C7$ is twice as much as that of the intra-cluster distances of $C2$. Thus the post PCA data is more suited to a K-means objective. We believe this is a good explanation on the comments by (KAH19).

Secondly, as we have discussed in Section 2.1.1, we observe that because of difference in pre PCA distances, post PCA average “intra cluster” distances of one cluster may become very similar to post PCA “inter cluster distance of other cluster”. This happens for $C4$ and $C7$ in the second dataset. In such a situation, it may appear PCA does not improve the dataset. However, if we use compression ratio as a metric, then the intra-cluster pairs of $C4$ have a comparatively higher ratio.

Here cluster $C8$ of Table 2 is the set of points that are unidentified, that is, their true labels are not known. They are essentially a mixture of different kinds of cells, and thus the fact that they have almost same intra-cluster and inter-cluster compression ratio aligns with our understanding of PCA.

Cluster name and size	Inter cluster Metric			Intra cluster Metric		
	pre-PCA average distance	post-PCA average distance	Compression Ratio	pre-PCA average distance	post-PCA average distance	Compression Ratio
$C1$ (933):	137.327	81.767	1.906	130.786	43.312	3.811
$C2$ (303):	115.654	71.037	1.96	74.939	21.46	4.431
$C3$ (638):	126.501	86.391	1.729	60.701	16.196	4.489
$C4$ (793):	134.3	77.361	2.019	135.08	61.86	2.847

Table 1: Relative compression on dataset 1 (KMA⁺15) with first 25 PCs

Cluster name and size	Inter cluster Metric			Intra cluster Metric		
	pre-PCA average distance	post-PCA average distance	Compression Ratio	pre-PCA average distance	post-PCA average distance	Compression Ratio
$C1$ (43):	566.672	361.345	1.622	432.565	82.812	6.398
$C2$ (761):	501.513	239.590	2.221	471.517	165.741	3.245
$C3$ (29):	587.985	381.784	1.600	459.003	116.707	5.220
$C4$ (812):	504.473	244.423	2.212	468.231	161.417	3.258
$C5$ (38):	559.504	350.365	1.649	436.998	103.031	5.978
$C6$ (22):	555.555	327.464	1.767	442.992	66.570	7.428
$C7$ (22):	588.917	412.013	1.471	390.259	57.708	7.588
$C8^*$ (82):	510.391	277.429	2.053	504.859	297.898	2.113

Remark: $C8$ is the collection of unidentified cells, which is not a real cluster

Table 2: Relative compression on dataset 2 (TMN⁺16) with first 25 PCs

Finally we finish this section with a discussion on the centering step that is conventionally applied prior to PCA in single-cell datasets, and how it fits into our model.

2.3 A note on centering

In this paper we have focused on uncentered-PCA. Let \hat{A} and \bar{A} be the uncentered and centered datasets. Then centered-PCA projects along the eigenvectors of $\bar{A}(\bar{A})^T$, whereas uncentered-PCA projects along the vectors of $\hat{A}\hat{A}^T$. The objective behind centering is so that the principle components are in the directions that minimize the sum of squared error with respect to the data mean.

We interpret this difference in terms of the Eigenbasis of the matrices. Let $\mathbf{c}_m \in \mathbb{R}^d$ be the column vector whose each entry is the mean of the corresponding rows. Then we can write

$$\bar{A}(\bar{A})^T = \hat{A}\hat{A}^T - \mathbf{c}_m(\mathbf{c}_m)^T$$

Now let us assume the top eigenvector of $\hat{A}\hat{A}^T$ and \mathbf{c}_m are colinear. Then the i -th eigenvector of $\bar{A}(\bar{A})^T$ is the same as the $(i + 1)$ -th eigenvector of $\hat{A}\hat{A}^T$, and they share the same eigenvalue. In

that case the analysis for $\overline{A}(\overline{A})^T$ for relative compression remains unchanged. This is what happens in the theoretical SBM model. In practice, we observe that the principle component of uncentered-PCA is “almost” colinear with \mathbf{c}_m , resulting in very similar compressibility results for uncentered and centered PCA which we demonstrate in Section 4.3. Now we describe our main theoretical proof in the next section.

3 Theoretical model and compression bounds

As we have discussed, the notion of clustering in our problem is the Euclidean distance, also called the ℓ_2 norm distance. For each $\mathbf{u}, \mathbf{v} \in \mathbb{R}^d$, their distance is defined as $\|\mathbf{u} - \mathbf{v}\| = \sqrt{\sum_{\ell=1}^d (\mathbf{u}_\ell - \mathbf{v}_\ell)^2}$.

3.1 More notations and preliminaries

For the matrices and vectors we use the following notations.

- We denote the random matrix representing the dataset by \hat{A} . If each column (datapoint) of \hat{A} is replaced by the center of the corresponding cluster, we obtain the center matrix A , which we also denote as the mean-matrix.
- We always denote columns with the subscript i and row with the subscript ℓ . Furthermore we denote the cluster identities with the subscript j .

Next we describe the norm definitions. We use the notation $\|\cdot\|$ in two sense. When the operand is a vector, it implies the ℓ_2 norm. When the operand is a matrix, it implies the *spectral* norm,

$$\|A\| = \arg \max_{v, \|v\| \leq 1} \{ \|Av\| \}$$

Having fixed our notations, we now move towards proving Theorem 1.

3.2 Proof of Theorem 1

Proving Theorem 1 constitutes proving the bounds on pre PCA (Numerators of Equations (1) and (2)) and the post PCA (Denominators of Equations (1) and (2)) intra and inter cluster distances.

We first concentrate on the pre PCA distances, which is simple to obtain. As the random variables (distributions) defining the vectors are all independent, the result follows from a simple application of the Hoeffding inequality.

Lemma 1. *Let \mathbf{u}_i and $\mathbf{u}_{i'}$ be two vectors (datapoints) of \hat{A} with ground truth clusters V_j and $V_{j'}$ respectively. If $j = j'$ then we have $\|\mathbf{u}_i - \mathbf{u}_{i'}\| \geq \sqrt{2d\sigma_j^2 - 12\sqrt{d}\log n}$ with probability $1 - \mathcal{O}(n^{-3})$, otherwise if $j \neq j'$ then we have $\|\mathbf{u}_i - \mathbf{u}_{i'}\| \leq \sqrt{d(\sigma_j^2 + \sigma_{j'}^2) + \|c_j - c_{j'}\|^2 + 12\sqrt{d}\log n}$ with probability $1 - \mathcal{O}(n^{-3})$.*

Proof. First we consider the case when \mathbf{u}_i and $\mathbf{u}_{i'}$ belong to the same cluster. Then $\|\mathbf{u}_i - \mathbf{u}_{i'}\|^2 = \sum_{\ell=1}^d ((\mathbf{u}_i)_\ell - (\mathbf{u}_{i'})_\ell)^2$ Here for each ℓ we define $\mathbf{w}_\ell = (\mathbf{u}_i)_\ell - (\mathbf{u}_{i'})_\ell = (c_j)_\ell + (\mathbf{e}_i)_\ell - (c_j)_\ell - (\mathbf{e}_{i'})_\ell = (\mathbf{e}_i)_\ell - (\mathbf{e}_{i'})_\ell$. Then $\mathbb{E}[\mathbf{w}_\ell^2] = \mathbb{E}[(\mathbf{e}_i)_\ell^2] + \mathbb{E}[(\mathbf{e}_{i'})_\ell^2] = \text{Var}((\mathbf{e}_i)_\ell) + \text{Var}((\mathbf{e}_{i'})_\ell)$.

We define $\sigma_{i,i}^2 = \text{Var}((\mathbf{e}_i)_\ell)$ (to use the more familiar row major representation). Recall that both \mathbf{e}_i and $\mathbf{e}_{i'}$ are sampled from $\mathcal{D}^{(j)}$ and σ_j^2 is the average of variance of the coordinates of the distribution $\mathcal{D}^{(j)}$. i.e., $\mathbb{E}[\sum_{\ell} \mathbf{w}_\ell^2] = \sum_{\ell=1}^d \sigma_{i,i}^2 + \sigma_{i,i'}^2 = 2d\sigma_j^2$ and applying Hoeffding bound on this setup we get

$$\Pr \left[\sum_{\ell=1}^d \mathbf{w}_\ell^2 \leq 2d\sigma_j^2 - 12\sqrt{d}\log n \right] \leq n^{-3}.$$

Thus, if \mathbf{u}_i and $\mathbf{u}_{i'}$ belong to the same cluster then with probability $1 - \mathcal{O}(n^{-3})$ we have $\|\mathbf{u}_i - \mathbf{u}_{i'}\| \geq \sqrt{2d\sigma_j^2 - 12\sqrt{d}\log n}$.

Similarly, if \mathbf{u}_i and $\mathbf{u}_{i'}$ belong to different clusters V_j and $V_{j'}$, we have the random variable $\mathbf{w}_\ell = (\mathbf{u}_i)_\ell - (\mathbf{u}_{i'})_\ell$ with mean $(c_j)_\ell - (c_{j'})_\ell$ (due to the difference in the cluster centers) and variance $\sigma_{\ell,i}^2 + \sigma_{\ell,j'}^2$, where we define $c_{\ell,j} = (c_j)_\ell$. Then $\mathbb{E}[\mathbf{w}_\ell^2] = \sigma_{\ell,i}^2 + \sigma_{\ell,j}^2 + (c_{\ell,j} - c_{\ell,j'})^2$ and

$$\mathbb{E}\left[\sum_{\ell=1}^d \mathbf{w}_\ell^2\right] = \sum_{\ell=1}^d \sigma_{\ell,i}^2 + \sigma_{\ell,j}^2 + (c_{\ell,j} - c_{\ell,j'})^2 = d(\sigma_j^2 + \sigma_{j'}^2) + \|c_i - c_{i'}\|^2$$

Applying Hoeffding bound we get

$$\Pr\left[\sum_{\ell=1}^d \mathbf{w}_\ell^2 \geq d(\sigma_j^2 + \sigma_{j'}^2) + \|c_j - c_{j'}\|^2 + 12\sqrt{d}\log n\right] \leq n^{-3}.$$

Thus if \mathbf{u}_i and $\mathbf{u}_{i'}$ belong to different clusters then with probability $1 - n^{-3}$ we have $\|\mathbf{u}_i - \mathbf{u}_{i'}\| \leq \sqrt{d(\sigma_j^2 + \sigma_{j'}^2) + \|c_j - c_{j'}\|^2 + 12\sqrt{d}\log n}$. □

Next, we prove the effect of PCA on these intra-cluster and inter-cluster distances, using concepts of random matrix theory and matrix perturbation theory.

3.3 Towards Post PCA distance

In this section we obtain bounds on the inter-cluster and intra-cluster distances after PCA is applied to the dataset. We first obtain some results on the behavior of random matrices and singular vectors that we use to obtain the said bounds.

3.3.1 A comparable symmetric case

The matrices of interest in our problem A and \hat{A} are non-symmetric and generally rectangular ($d \times n$). To be able to use the deeper theoretical understanding of symmetric random matrices as opposed to non-symmetric ones, we define a comparable symmetric matrix to better analyze the behavior of the principle components of \hat{A} . Corresponding to A and \hat{A} we define the $(d+n) \times (d+n)$ matrices $B = \begin{bmatrix} 0 & A \\ A^T & 0 \end{bmatrix}$ and $\hat{B} = \begin{bmatrix} 0 & \hat{A} \\ \hat{A}^T & 0 \end{bmatrix}$ which are both symmetric. We also define $E_B = B - \hat{B}$. Then the eigenvectors of \hat{B} and singular vectors of \hat{A} (and similarly B and A) are related as follows.

Fact 1. *Let the left and right singular vectors of \hat{A} be $\hat{\mathbf{l}}_t, 1 \leq t \leq d$ and $\hat{\mathbf{r}}_t, 1 \leq t \leq n$ respectively. Then the eigenvectors of \hat{B} (that form orthonormal columns) are $\frac{1}{\sqrt{2}} \begin{bmatrix} \hat{\mathbf{l}}_t \\ \hat{\mathbf{r}}_t \end{bmatrix}$ with eigenvalue $\hat{\lambda}_t = s_t$ and $\frac{1}{\sqrt{2}} \begin{bmatrix} \hat{\mathbf{l}}_t \\ -\hat{\mathbf{r}}_t \end{bmatrix}$ with eigenvalue $\hat{\lambda}_t = -s_t$ where $1 \leq t \leq \min(d, n)$. The same follows for A and B .*

Here we also formally define P_B^k for symmetric matrices as in this case we work with eigenvectors corresponding to top eigenvalues, instead of top singular values (as in case of A), for clarity.

Remark 3. *For the $d \times n$ matrix A (and similarly for \hat{A}) we have defined P_A^k as the matrix whose rows are the top k singular vectors of A .*

When we discuss a symmetric matrix B , P_B^k is a matrix whose rows are the eigenvectors corresponding to the top k eigenvalues of B .

Now we use the Davis-Kahan Theorem (DK70) along with a result from Cape et. al. (CTP19) to obtain an upper bound between the norm of difference of eigenvectors of B and \hat{B} under some appropriate orthonormal rotation that we shall use to obtain our results.

Theorem 2 (Davis-Kahan Theorem: (DK70)). *Let D and \hat{D} be $p \times p$ symmetric matrices, with eigenvalues $\lambda_1, \dots, \lambda_p$ and $\hat{\lambda}_1, \dots, \hat{\lambda}_p$ respectively. Define $E_D = \hat{D} - D$ and $\delta_k = \lambda_k - \lambda_{k+1}$, $1 \leq k < p$. Let $U = [\mathbf{u}_1 \dots \mathbf{u}_k]$ and $\hat{U} = [\hat{\mathbf{u}}_1 \dots \hat{\mathbf{u}}_k]$ are orthonormal matrices in $\mathbb{R}^{p \times k}$ where \mathbf{u}_i and $\hat{\mathbf{u}}_i$ are eigenvectors of D and \hat{D} w.r.t to the i -th top eigenvalue. Then*

$$\left\| \sin \Theta \left(U, \hat{U} \right) \right\| \leq \frac{2 \|E_D\|}{\delta_k} \quad (3)$$

Theorem 3 (Perturbation under Procrustes Transformation: (CTP19)). *Given two sets of $p \times k$ orthonormal matrices U and \hat{U} , there exists a $k \times k$ orthonormal matrix W_U such that*

$$\left\| \sin \Theta \left(U, \hat{U} \right) \right\| \leq \|U - \hat{U}W_U\| \leq \sqrt{2} \left\| \sin \Theta \left(U, \hat{U} \right) \right\|$$

Combining them we get the following result.

Theorem 4. *Given the matrices A and \hat{A} and B and \hat{B} defined as described above, there exists an orthonormal matrix W_B such that*

$$\left\| (P_B^k)^T - (P_{\hat{B}}^k)^T W \right\| \leq \frac{2 \|E_B\|}{s_k}$$

Finally, we bound the term $\|E_B\|$, which is a direct corollary of Vu (VU18)[Lemma 8].

Theorem 5 (Norm of random symmetric matrix (VU18)). *Let E be a $n \times n$ random symmetric matrix where each entry in the upper diagonal is an independent random variable with 0 mean and σ variance, then there is a constant C_0 such that*

$$\Pr \left[\|E\| \geq C_0 \sigma \sqrt{n} \right] \leq n^{-3}$$

where $\sigma \geq C_0 \frac{\log n}{n}$.

Now we setup some of the bounds that we will use to complete the post PCA distance bounds.

3.3.2 Random Projection

Here we derive a bound for $\|P_C^k e\|$ where $e \in \mathbb{R}^d$ is a coordinate wise independent random vector with mean 0. Here an important condition is that C and e are independent.

The projection matrix P_C^k is a set of k -orthonormal unit vectors \mathbf{p}_t , $1 \leq t \leq k$.

Then the length of a projected vector $\|P_C^k e\|$ can be written down as

$$\|P_C^k e\|^2 = \sum_{t=1}^k \left((\mathbf{p}_t)^T e \right)^2$$

We first concentrate on the individual dot-products in the following lemma, closely following the random projection idea by Vu (VU18).

Lemma 2. *Let e be a d -dimensional random vector with 0-mean entries and maximum variance σ^2 . Then for any unit vector \mathbf{v} so that e and \mathbf{v} are independent of each other we have $\Pr \left[-\sigma - \alpha \leq (\mathbf{v})^T e \leq \sigma + \alpha \right] \geq 1 - e^{-\alpha^2/4}$*

Proof. The function $(\mathbf{v})^T e$ is a 1-Lipschitz convex function for any unit vector \mathbf{v} , and thus Talagrand's inequality gives us $\Pr \left[|(\mathbf{v})^T e - \mathbb{E}[(\mathbf{v})^T e]| \geq +\alpha \right] \leq e^{-\alpha^2/4}$.

We then bound $\mathbb{E}[(\mathbf{v})^T e]^2$. We have

$$\begin{aligned} \mathbb{E}[(\mathbf{v})^T e]^2 &= \mathbb{E} \left[\left(\sum_{\ell=1}^d \mathbf{v}_\ell e_\ell \right)^2 \right] = \mathbb{E} \left[\sum_{i_1=1}^d \sum_{i_2=1}^d \mathbf{v}_{i_1} e_{i_1} \mathbf{v}_{i_2} e_{i_2} \right] = \mathbb{E} \left[\sum_{\ell=1}^d (\mathbf{v}_\ell e_\ell)^2 \right] \\ &\leq \sigma^2 \sum_{\ell=1}^d \mathbf{v}_\ell^2 \\ &\leq \sigma^2 \end{aligned}$$

Thus we have $\mathbb{E}[(\mathbf{v}^T \mathbf{e})^2] \leq \sigma^2$. Now using Jensen's inequality we have $(E[X])^2 \leq E[X^2]$ and thus $-\sigma \leq \mathbb{E}[(\mathbf{v}^T \mathbf{e})] \leq \sigma$, which completes the proof. \square

Having analyzed the projection due to one singular (eigen) vector, we now extend it to k vectors.

Lemma 3. *Let $P_{\hat{A}}^k$ be a $k \times d$ orthonormal matrix and \mathbf{e} be a d -dimensional random vector with each entry having zero mean and variance at most σ^2 . Then with probability $1 - (nk)^{-c_0+1}$ we have,*

$$\|P_{\hat{A}}^k(\mathbf{e})\| \leq \sqrt{k}(\sigma + \sqrt{4c_0 \log(nk)})$$

where $P_{\hat{A}}^k$ and \mathbf{e}_i are independent.

Proof. Let the k -many d -dimensional eigenvectors of $P_{\hat{A}}^k$ be $\mathbf{p}_t, 1 \leq t \leq k$. We denote $F_t = ((\mathbf{p}_t)^T \mathbf{e})^2$. Then from Lemma 2 we have $\Pr(F_t \geq (\sigma + \sqrt{4c_0 \log(nk)})^2) \leq (nk)^{-c_0}, c_0 > 1$.

Let the event $F_t \geq (\sigma + \sqrt{4c_0 \log(nk)})^2$ be E_t . Then by union bound we have $\Pr[\cup_{t=1}^k E_t] \leq k \cdot (nk)^{-c_0} \leq (nk)^{-c_0+1}$. \square

Having established these results, now we can analyze the post-PCA intra-cluster and inter-cluster bounds.

3.3.3 Post PCA Intra-cluster Distance

Now we obtain the post-PCA distance $\|P_{\hat{A}}^k(\mathbf{u}_i - \mathbf{u}_{i'})\|$ where $\mathbf{u}_i, \mathbf{u}_{i'} \in V_j$ belong to the same cluster V_j .

Lemma 4. *Let \mathbf{u}_i and $\mathbf{u}_{i'}$ be two columns of the data matrix \hat{A} belonging to the same cluster V_j . Then for some constant C_0 we have*

$$\|P_{\hat{A}}^k(\mathbf{u}_i - \mathbf{u}_{i'})\| \leq 2\sqrt{2} \left(\sqrt{k} \left(\sigma + \sqrt{16 \log(nk)} \right) + \frac{C_0 \sigma \sigma_j \sqrt{d(d+n)}}{s_k} \right)$$

with probability $1 - \mathcal{O}(n^{-3})$.

Proof. The vectors can be described as $\mathbf{u}_i - \mathbf{u}_{i'} = c_j + \mathbf{e}_i - c_j - \mathbf{e}_{i'} = \mathbf{e}_i - \mathbf{e}_{i'}$. Therefore

$$\|P_{\hat{A}}^k(\mathbf{u}_i - \mathbf{u}_{i'})\| = \|P_{\hat{A}}^k(\mathbf{e}_i - \mathbf{e}_{i'})\| \leq 2\|P_{\hat{A}}^k(\mathbf{e}_i)\|$$

This is because \mathbf{e}_i and $\mathbf{e}_{i'}$ are two i.i.d samples drawn from $\mathcal{D}^{(j)}$. Now we analyze $\|P_{\hat{A}}^k(\mathbf{e}_i)\|$ using the matrices B and \hat{B} . We have $\|P_{\hat{A}}^k(\mathbf{e}_i)\| = \sqrt{2} \left\| \left(P_{\hat{B}}^k \right)^T \begin{bmatrix} \mathbf{e}_i \\ 0^n \end{bmatrix} \right\|$ from Fact 1. Denote $\mathbf{e}_i|0^n = \begin{bmatrix} \mathbf{e}_i \\ 0^n \end{bmatrix}$.

Then $\mathbf{e}_i|0^n$ is a $(d+n)$ -dimensional random vector whose each entry is independent zero mean and has variance at most σ . Here it should be noted that we cannot analyze $P_{\hat{B}}^k(\mathbf{e}_i|0^n)$ directly using Lemma 3, since $\mathbf{e}_i|0^n + c_j|0^n$ is a vector in \hat{B} , and thus the entries of $P_{\hat{B}}^k$ and $\mathbf{e}_i|0^n$ are not independent of each other. We instead use the corresponding mean-matrix (center-matrix) B as follows.

$$\begin{aligned} \|P_{\hat{B}}^k(\mathbf{e}_i|0^n)\| &= \|(P_{\hat{B}}^k - WP_{\hat{B}}^k)(\mathbf{e}_i|0^n) + WP_{\hat{B}}^k(\mathbf{e}_i|0^n)\| \\ &\leq \|(P_{\hat{B}}^k - WP_{\hat{B}}^k)\| \cdot \|\mathbf{e}_i|0^n\| + \|WP_{\hat{B}}^k(\mathbf{e}_i|0^n)\| \end{aligned}$$

where W is any $k \times k$ orthonormal matrix. Then we get $\|WP_{\hat{B}}^k(\mathbf{e}_i|0^n)\| = \|P_{\hat{B}}^k(\mathbf{e}_i|0^n)\| \leq \sqrt{k} \left(\sigma + \sqrt{16 \log(nk)} \right)$ with probability $1 - (nk)^{-3}$ by applying Lemma 3 with $c_0 = 4$.

We also have $\|\mathbf{e}_i|0^n\| \leq 3\sigma\sqrt{d}$ with probability $1 - \mathcal{O}(n^{-3})$ as a corollary of Lemma 1.

Finally we analyze the first term. We have

$$\|(P_{\hat{B}}^k - WP_{\hat{B}}^k)\| = \left\| \left(P_{\hat{B}}^k - WP_{\hat{B}}^k \right)^T \right\| = \left\| \left((P_{\hat{B}}^k)^T - (P_{\hat{B}}^k)^T W^T \right) \right\|$$

From the definition of P^k for symmetric matrices, we have $(P_{\hat{B}}^k)^T = \hat{U}$ and $(P_B^k)^T = U$, where \hat{U} and U are the top k eigen valued eigenvectors of B and \hat{B} respectively. Thus, applying Theorem 4 and setting $W^T = W_B$ we get $\|P_{\hat{B}}^k - WP_B^k\| \leq \frac{2\|E_B\|}{s_k}$, where E_B is a $(d+n) \times (d+n)$ symmetric matrix whose each entry is a zero mean independent random variable with variance at most σ . Using Theorem 5 we get $\|E_B\| \leq C_0\sigma\sqrt{d+n}$ with probability $1 - \mathcal{O}(n^{-3})$. Combining the results we get

$$\|P_{\hat{B}}^k(\mathbf{e}_i|0^n)\| \leq \frac{C_0\sigma\sigma_j\sqrt{d(d+n)}}{s_k} + \sqrt{k} \left(\sigma + \sqrt{16 \log(nk)} \right)$$

with probability $1 - \mathcal{O}(n^{-3})$. This completes the proof. \square

Let us now observe the distances between vectors in different clusters, which is obtained in a very similar manner.

3.3.4 Post PCA Inter-cluster distance

Lemma 5. *Let $\mathbf{u}_i, \mathbf{u}_{i'}$ be two columns of the data matrix hA so that $\mathbf{u}_i \in V_j$ and $\mathbf{u}_{i'} \in V_{j'}$ in our clustering model, where $j \neq j'$. Then for some constant C_0 we have*

$$\begin{aligned} & \|P_{\hat{A}}^k(\mathbf{u}_i - \mathbf{u}_{i'})\| \\ & \geq \|c_j - c_{j'}\| - 2\sqrt{k} \left(\sigma + \sqrt{16 \log(nk)} \right) - \frac{2C_0\sigma^2 \sqrt{2(d+n)} (\|c_j - c_{j'}\|^2 + d(\sigma_j^2 + \sigma_{j'}^2))}{s_k} \end{aligned}$$

with probability $1 - \mathcal{O}(n^{-3})$.

Proof. As before, for any vector \mathbf{u} , we define $\mathbf{u}|0^n = \begin{bmatrix} \mathbf{u} \\ 0^n \end{bmatrix}$. As in Lemma 4, $\|P_{\hat{A}}^k(\mathbf{u}_i - \mathbf{u}_{i'})\| = \sqrt{2} \left\| P_{\hat{B}}^k(\mathbf{u}_i|0^n - \mathbf{u}_{i'}|0^n) \right\|$. Also, $\|P_{\hat{B}}^k(\mathbf{u}_i|0^n - \mathbf{u}_{i'}|0^n)\| = \|P_{\hat{B}}^k(c_j|0^n - c_{j'}|0^n + \mathbf{e}_i|0^n - \mathbf{e}_{i'}|0^n)\|$ where c_j and $c_{j'}$ are the mean vectors corresponding to the clusters V_j and $V_{j'}$. Thus c_j and $c_{j'}$ are two columns of A . Then we have

$$\begin{aligned} & \|P_{\hat{B}}^k(\mathbf{u}_i|0^n - \mathbf{u}_{i'}|0^n)\| \\ & \geq \|P_{\hat{B}}^k(c_j|0^n - c_{j'}|0^n + \mathbf{e}_i|0^n - \mathbf{e}_{i'}|0^n)\| - \|(P_{\hat{B}}^k - P_B^k)(\mathbf{u}_i|0^n - \mathbf{u}_{i'}|0^n)\| \\ & \geq \|P_{\hat{B}}^k(c_j|0^n - c_{j'}|0^n + \mathbf{e}_i|0^n - \mathbf{e}_{i'}|0^n)\| - \|(P_{\hat{B}}^k - P_B^k)\| \cdot \|\mathbf{u}_i|0^n - \mathbf{u}_{i'}|0^n\| \\ & \geq \|P_B^k(c_j|0^n - c_{j'}|0^n)\| - \|P_B^k(\mathbf{e}_i|0^n - \mathbf{e}_{i'}|0^n)\| - \|(P_{\hat{B}}^k - P_B^k)\| \cdot \|\mathbf{u}_i|0^n - \mathbf{u}_{i'}|0^n\| \end{aligned}$$

The top k -eigenvectors of B can be described as $\mathbf{b}_t = \begin{bmatrix} \mathbf{l}_t \\ \mathbf{r}_t \end{bmatrix}$ where \mathbf{l}_t and \mathbf{r}_t are the left and right singular vectors of A . Thus we have $\|P_B^k(c_j|0^n - c_{j'}|0^n)\| = \|c_j - c_{j'}\|$.

From Lemma 3 we have $\|P_{\hat{B}}^k(\mathbf{e}_i|0^n - \mathbf{e}_{i'}|0^n)\| \leq 2\sqrt{k}(\sigma + \sqrt{16 \log(nk)})$ with probability $1 - \mathcal{O}(n^{-3})$.

Finally, following Lemma 4 with probability $1 - \mathcal{O}(n^{-3})$ we have

$$\|(P_{\hat{B}}^k - P_B^k)\| \cdot \|\mathbf{u}_i|0^n - \mathbf{u}_{i'}|0^n\| \leq \frac{2C_0\sigma^2\sqrt{d+n}\sqrt{2\|c_j - c_{j'}\|^2 + d(\sigma_j^2 + \sigma_{j'}^2)}}{s_k}$$

Combining these bounds, we have

$$\begin{aligned} & \|P_{\hat{B}}^k(\mathbf{u}_i|0^n - \mathbf{u}_{i'}|0^n)\| \\ & \geq \|P_B^k(c_j|0^n - c_{j'}|0^n)\| - \|P_B^k(\mathbf{e}_i|0^n - \mathbf{e}_{i'}|0^n)\| - \|(P_{\hat{B}}^k - P_B^k)\| \cdot \|\mathbf{u}_i|0^n - \mathbf{u}_{i'}|0^n\| \\ & \geq \|c_j - c_{j'}\| - 2 \left(\sqrt{k} \left(\sigma + \sqrt{16 \log(nk)} \right) - \frac{2C_0\sigma^2 \sqrt{2(d+n)} (\|c_j - c_{j'}\|^2 + d(\sigma_j^2 + \sigma_{j'}^2))}{s_k} \right) \end{aligned}$$

with probability $1 - \mathcal{O}(n^{-3})$. Lastly, we use that $\|P_{\hat{A}}^k(\mathbf{u}_i - \mathbf{u}_{i'})\| = \sqrt{2} \left\| P_{\hat{B}}^k(\mathbf{u}_i|_{0^n} - \mathbf{u}_{i'}|_{0^n}) \right\|$ to get our bound. \square

Since we have all the bounds with for any pair with probability $1 - \mathcal{O}(n^{-3})$, a simple union bound gives us Theorem 1, where the bounds on k -PC compression bounds holds for all possible pairs of points, with probability $1 - \mathcal{O}(n^{-1})$.

3.4 Projection with more principle components

In our setup, clearly choosing the number of PCs k' to be equal to number of ground truth cluster k generates very good compression ratio. Since k is unknown, it is important to understand what happens when $k' \neq k$.

The main challenge in theoretically proving our bounds for $k' \neq k$ comes from Theorem 4. We recall the result, which states

$$\left\| (P_{\hat{B}}^{k'})^T - (P_B^{k'})^T W \right\| \leq \frac{2\|E_B\|}{s_{k'}}$$

In general we work with the natural assumption $s_k \gg \|E\|$. However, in our model we have $s_{k+1} = \mathcal{O}(\|E\|)$. This follows from Weyl's inequality, which states that if $\hat{B} = B + E_B$ and $(k+1)$ -th singular value of B is 0, then $(k+c)$ -th singular value of \hat{B} is upper bounded by $\mathcal{O}(\|E\|)$ for any $c > 0$. This means we get $\left\| (P_{\hat{B}}^{k'})^T - (P_B^{k'})^T W \right\| = \Omega(1)$, and thus $P_{\hat{A}}^k(\mathbf{u}_i - \mathbf{u}_{i'}) = \Omega(\sigma\sqrt{d})$, and the intra-cluster compression ratio becomes less than 2.

In this section we bypass this issue to a lose but non-trivial extent by separately considering $P_{\hat{A}}^{(k+1, k')}(\mathbf{u}_i - \mathbf{u}_{i'})$, which is the projection due to the $k+1$ to k' -th PCs (left singular vectors of \hat{A}). We provide some theoretical evidence that even if we choose $k' = k+c$ where c is a constant, the compression ratio is still good. We observe the singular value decomposition of \hat{A} .

Since $k' > k$, we have $\|P_{\hat{A}}^{k'}(\mathbf{u}_i - \mathbf{u}_{i'})\| \geq \|P_{\hat{A}}^k(\mathbf{u}_i - \mathbf{u}_{i'})\|$ for any pair of vectors $\mathbf{u}_i, \mathbf{u}_{i'}$ and thus the upper bound on the K -PC inter cluster compression still holds.

Now we concentrate on the intra-cluster bounds, and how the following result.

Lemma 6. *Let $k' = k+c$ and $f < 1$ and C_0 be the constant as defined in Theorem 5. Then for for all but $\mathcal{O}\left(\frac{c^2}{f^4}\right)$ pairs of intra cluster points we have*

$$P_{\hat{A}}^{k'}(\mathbf{u}_i - \mathbf{u}_{i'}) \leq \sqrt{\left\| P_{\hat{A}}^k(\mathbf{u}_i - \mathbf{u}_{i'}) \right\|^2 + C_0^2 \sigma^2 (d+n) c^2 f^2}$$

Proof. We bound $P_{\hat{A}}^{(k+1, k')}(\mathbf{u} - \mathbf{v})$, which is the projection due to the $k+1$ to k' -th PCs (left singular vectors of \hat{A}).

We can write $\hat{A} = \sum_{\ell=1}^{n'} s_{\ell} \mathbf{l}_{\ell} (\mathbf{r}_{\ell})^T$ where $s_{\ell}, \mathbf{l}_{\ell}$ and \mathbf{r}_{ℓ} are the ℓ -th singular value, left singular vector and right singular vector respectively, and $n' = \min(d, n)$.

Let \mathbf{u}_i be the i -th column vector of \hat{A} . Then the projection of \mathbf{u}_i due to the ℓ -th principle component is $\langle \mathbf{l}_{\ell}, \mathbf{u}_i \rangle = s_{\ell} r_{\ell, i}$ where $r_{\ell, i}$ is the i -th coordinate of the ℓ -th right singular vector. Thus, if we consider $P_{\hat{A}}^{(k+1, k')}$ for all the vectors $\mathbf{u} \in \hat{A}$, it gives us a $c \times n$ matrix \hat{A}_c , where the t -th row is $[s_{k+t} r_{k+t, 0}, s_{k+t} r_{k+t, 1}, \dots, s_{k+t} r_{k+t, n-1}]$, where we have $s_{k+t} \leq C_0 \sigma \sqrt{d+n}$. This is because $\hat{A} = A + \|E\|$, and A is rank k , where $\|E\|$ (the norm or top singular value of E) is upper bounded by $C_0 \sigma \sqrt{d+n}$. Applying Weyl's inequality gives us $s_{k+t} \leq C_0 \sigma \sqrt{d+n}$.

Now, since the right singular vectors are unit vectors, we have $\sum_{i=1}^n (r_{k+t, i}^2) = 1$.

Thus, for any row the number of entries of \hat{A}_c that can be larger than $s_t f$ for any $f < 1$ is $\mathcal{O}((1/f)^2)$. Then for any f , the total number of entries larger than $C_0 \sigma (\sqrt{d+n}) f$ in \hat{A}_c

is upper bounded by $\mathcal{O}\left(\frac{c}{f^2}\right)$. This implies that the total number of pairs of points for which $\|P_{\hat{A}}^{(k+1,k')}(\mathbf{u}_i - \mathbf{u}_{i'})\| > C_0 c \sigma (\sqrt{d+n}) f$ is upper bounded by $\mathcal{O}\left(\frac{c^2}{f^4}\right)^2$.

Since $\|P_{\hat{A}}^{k'}(\mathbf{u}_i - \mathbf{u}_{i'})\| = \sqrt{\|P_{\hat{A}}^k(\mathbf{u}_i - \mathbf{u}_{i'})\|^2 + \|P_{\hat{A}}^{k+1,k'}(\mathbf{u}_i - \mathbf{u}_{i'})\|^2}$ this completes the proof. \square

For example, if we fix $f = \frac{1}{\log n}$ then at most $c^2 \log n^4$ of the intra-cluster pairs will have more than $\frac{\sigma \sqrt{d+n}}{\log n}$ post-PCA distance. Then the intra-cluster post-PCA $(k+c)$ -PC compression is still lower bounded by $\log n$ for all but $c^2 \log n^4$ of the pairs.

It should be noted that this is a much looser bound as compared to our k -PC compression metric, especially in the paradigm where noise dominates the ground truth distances. As we discussed, the main reason that Theorem 1 does not directly work for $k' > k$ can be pinned down to a technical challenge.

3.4.1 Technical challenges and opportunities in understanding PCA

The technical challenge is getting a better upper bound on $\|(P_{\hat{B}}^k - P_B^k)(e)\|$ than $\|P_{\hat{B}}^k - P_B^k\| \cdot \|e\|$. In fact, $\|(P_{\hat{B}}^k - P_B^k)e\|$ equals $\|(P_{\hat{B}}^k - P_B^k)\| \cdot \|e\|$ only if $e/\|e\|$ is a unit vector along which $(P_{\hat{B}}^k - P_B^k)$ realizes its spectral norm, which is unlikely to be the case for most noise e vectors, due to the inherent randomness in them. A better analysis of this term will allow us to extend the result of Theorem 1 beyond $k' = k$, which is what we observe in reality. For real datasets, the compression factor does not change much if the PCA dimension is changed by a small value. Furthermore, a tighter understanding of $\|(P_{\hat{B}}^k - P_B^k)e\|$ will also enable us to make progress towards proving optimality of perhaps the simplest spectral clustering algorithm for the SBM problem, as conjectured by (VU18). We leave this as an outstanding open question.

4 Experimental results

In Section 2.2, we have given initial evidence of PCA’s compressibility for the data two datasets that we have considered. Specifically, we observed the average inter and intra cluster distances for each cluster before and after PCA. Here we focus on dataset-2 ((TMN⁺16)) and demonstrate more detailed evidence that supports our analysis and model. We first show the average inter and intra cluster distance metrics for each cell. This is a more granular view of the distance metric, and gives us a better picture of PCA’s compressibility. Next we provide evidence to highlight the similarity of centered and uncentered PCA in terms of compressibility, and provide metric comparable to Tables 1 and 2. Finally, we calculate the average metrics when for dataset-2 when projection is done using different number of PCs, and observe how the metrics do not change drastically.

4.1 Cell wise average distances for

In our theoretical model, we proved in Theorem 1 that the k -PC compression ratio of “all” intra cluster pairs is better than that of “all” inter cluster ones. Then to support our hypothesis on, we described the average inter and intra cluster distances for each cluster of two datasets in Table 1 and Table 2. This is still a high level overview of PCA’s compressibility. Here we look at a more detailed, “cellwise” metric. For each cell(vector) $\mathbf{u} \in \hat{A}$ belonging to ground truth cluster V_j , we calculate its average intra cluster distance as $Avg(\mathbf{u})_{\text{intra}} = \mathbb{E}_{\mathbf{v} \in V_j} \left[\frac{\|\mathbf{u}-\mathbf{v}\|}{P_{\hat{A}}^k(\mathbf{u}-\mathbf{v})} \right]$. Similarly we calculate the average inter cluster distance as $Avg(\mathbf{u})_{\text{inter}} = \mathbb{E}_{\mathbf{v} \notin V_j} \left[\frac{\|\mathbf{u}-\mathbf{v}\|}{P_{\hat{A}}^k(\mathbf{u}-\mathbf{v})} \right]$. We note down the results for the cells in cluster 2 and 3 in Figure 1. We observe that almost all of the intra-cluster compression ratios are significantly larger than the inter-cluster ratios. The results for the other clusters are quite similar.

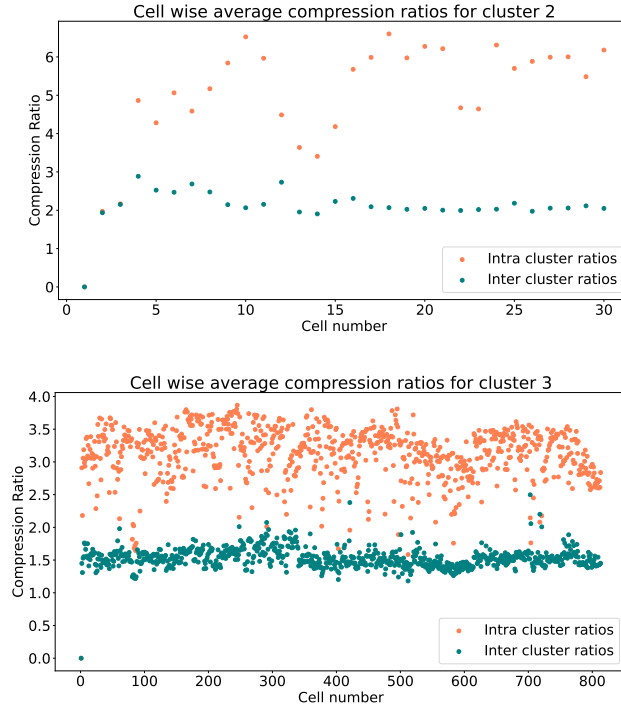


Figure 1: Cell wise average compression ratio for cluster C_2 and C_3 of dataset-2 (TMN⁺16) for 25 PCs

4.2 Cluster relations of pairs with highest compression

Next we describe another metric that highlights PCA's impact on the single-cell datasets. We draw a graph where the x -axis denotes the top x -fraction of the pairs sorted by highest to lowest compression ratio, and the corresponding y value denoted the fraction of those pairs that belong to the same cluster. For dataset-2, more than 98% of the top 10% pairs are intra-cluster pairs, and the fraction of intra-cluster pairs does not have a steep decline. This implies if one embeds the points onto a graph where there is an edge between a pair of nodes if their corresponding compression ratio is in the top 10%, then in the resulting graphs almost all the edges will be intra-cluster edges.

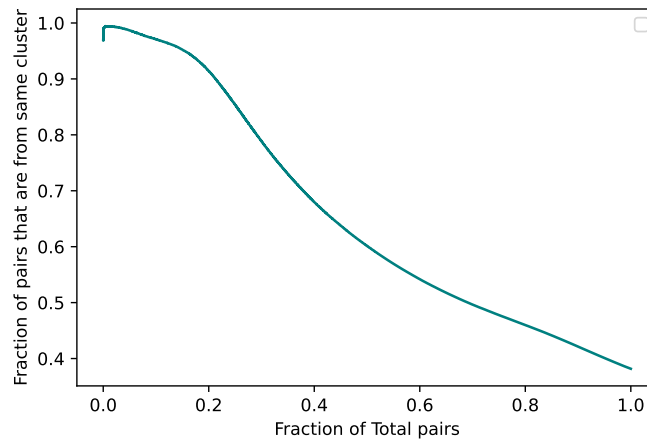


Figure 2:

4.3 Compression due to centered PCA

In Section 2.3 we discussed how the centered PCA use in practice has very similar compressibility to the uncentered version we analyze here. Here we verify that for dataset 2 where projection is done on 25 PCs. First, we describe the uncentered result again for ease of comparison.

Cluster name and size	Inter cluster Metric			Intra cluster Metric		
	pre-PCA average distance	post-PCA average distance	Compression Ratio	pre-PCA average distance	post-PCA average distance	Compression Ratio
C_1 (43):	566.672	361.345	1.622	432.565	82.812	6.398
C_2 (761):	501.513	239.590	2.221	471.517	165.741	3.245
C_3 (29):	587.985	381.784	1.600	459.003	116.707	5.220
C_4 (812):	504.473	244.423	2.212	468.231	161.417	3.258
C_5 (38):	559.504	350.365	1.649	436.998	103.031	5.978
C_6 (22):	555.555	327.464	1.767	442.992	66.570	7.428
C_7 (22):	588.917	412.013	1.471	390.259	57.708	7.588
C_{8^*} (82):	510.391	277.429	2.053	504.859	297.898	2.113

Table 3: Relative compression on dataset 2 (TMN⁺16) with first 25 PCs for uncentered PCA

Now let us look at the results for centered PCA. As one can see, the compression factors differ by at around a factor of 0.1, and for some clusters, it is as low as 0.01. This matches our theoretical understanding of centering from an Eigenbasis perspective.

Cluster name and size	Inter cluster Metric			Intra cluster Metric		
	pre-PCA average distance	post-PCA average distance	Compression Ratio	pre-PCA average distance	post-PCA average distance	Compression Ratio
C_1 (43):	566.672	361.671	1.620	432.565	83.513	6.523
C_2 (761):	501.513	240.050	2.216	471.517	166.299	3.231
C_3 (29):	587.985	382.274	1.597	459.003	118.102	5.362
C_4 (812):	504.473	244.890	2.207	468.231	162.040	3.243
C_5 (38):	559.504	350.983	1.645	436.998	104.907	6.065
C_6 (22):	555.555	327.969	1.764	442.992	67.609	7.678
C_7 (22):	588.917	412.022	1.471	390.259	57.385	8.024
C_{8^*} (82):	510.391	278.386	2.043	504.859	298.653	2.129

Table 4: Relative compression due to “Centered” PCA on dataset 2 (TMN⁺16) with first 25 PCs

4.4 Compression due to different Number of PCs

Finally, we address the fact that in reality one cannot know the exact number of ground truth cluster. In this direction we observe that the compressibility of PCA does not drastically vary with small change in the number of PCs. Dataset-2 has 8 primary clusters (with one comprising of unidentified cells). In this case, as observed from the experiments, starting from 10-PCs the compression ratio worsen (intra-cluster ratio decreases, and inter-cluster ratio increases) with increasing number of PCs, but the change is not slow, to the point that even for 35 PCs the intra cluster compression ratio is significantly higher than inter cluster compression ratio for most cluster. We have given a loose theoretical proof of this phenomenon in Section 3.4, but we believe a more robust proof, in line with practical observation is possible.

Cluster name and size	Inter cluster Metric			Intra cluster Metric		
	pre-PCA average distance	post-PCA average distance	Compression Ratio	pre-PCA average distance	post-PCA average distance	Compression Ratio
$C1$ (43):	566.672	349.476	1.710	432.565	73.806	8.082
$C2$ (761):	501.513	221.012	2.451	471.517	140.741	4.254
$C3$ (29):	587.985	352.592	1.847	459.003	91.159	7.454
$C4$ (812):	504.473	225.872	2.445	468.231	135.838	4.208
$C5$ (38):	559.504	331.114	1.781	436.998	85.474	7.913
$C6$ (22):	555.555	299.849	2.013	442.992	55.549	10.528
$C7$ (22):	588.917	383.527	1.692	390.259	48.958	10.315
$C8$ (82):	510.391	254.191	2.334	504.859	272.852	2.560

Table 5: Relative compression on dataset 2 (TMN⁺16) with first 10 PCs

Cluster name and size	Inter cluster Metric			Intra cluster Metric		
	pre-PCA average distance	post-PCA average distance	Compression Ratio	pre-PCA average distance	post-PCA average distance	Compression Ratio
$C1$ (43):	566.672	364.253	1.606	432.565	87.732	5.924
$C2$ (761):	501.513	246.330	2.147	471.517	176.089	2.961
$C3$ (29):	587.985	384.848	1.584	459.003	122.571	4.958
$C4$ (812):	504.473	251.025	2.138	468.231	169.991	3.025
$C5$ (38):	559.504	358.816	1.600	436.998	124.744	5.273
$C6$ (22):	555.555	332.190	1.736	442.992	73.423	6.767
$C7$ (22):	588.917	414.310	1.461	390.259	61.854	7.207
$C8$ (82):	510.391	285.121	1.974	504.859	305.251	2.033

Table 6: Relative compression on dataset 2 (TMN⁺16) with first 35 PCs

5 Conclusion

5.1 Compressibility and Seurat’s Performance

PCA’s compressibility also helps us understand reason behind success of heuristic single-cell clustering algorithm such as Seurat. The main steps of Seurat are applying a supervised variant of PCA on the data, followed by a embedding the dataset onto a 20-NN graph, where each node is connected to 20 nearest neighbours. Then in the final step Louvain algorithm is run on the graph, which is a heuristic local graph clustering algorithm.

The supervised variant of the PCA also has a compressibility factor similar to the uncentered PCA we have discussed here. From figure 2, we have observed that highly compressed pairs are likely to be the same cluster, which makes the 20-NN graph created by Seurat to be mostly populated by intra-cluster edges, and the output of the graph clustering algorithm then has high accuracy.

5.2 Towards better algorithms

In this section, we briefly discuss how our analysis may help to design vector clustering algorithms. We focus on single-cell analysis again. In single-cell analysis, it has been widely believed that PCA is just a dimensionality reduction tool, and the later clustering algorithm (such as graph clustering or K-means) is the main part of clustering. However, in this paper, we demonstrated that PCA itself is a very good clustering algorithm, and how it helps create a graph whose clustering has high accuracy.

Furthermore, hierarchical clustering is an important clustering paradigm for single-cell clustering, because of existence of complex sub-populations of cells with broader classification. For example, both T cells and B cells are immune cells. However, in one-level clustering such as Seurat CD4 memory cells and CD8 cytotoxic cells are clustered together when supplied in a mixture of

other kind of CD cells. Such scenarios are abundantly present in single-cell data, which increases the importance of better hierarchical clustering. As mentioned in (KAH19), existing hierarchical clustering are generally slow, and there is no good theoretic foundation.

In this direction, we observe that PCA's compression phenomenon is observed in many complicated combination of cells, and also within the sub-populations itself, and we aim to design better hierarchical algorithms in our next step.

Furthermore, the review paper (KAH19) discusses several challenges for this direction.

- How to validate the clustering result?
- How to implement faster algorithms as the data size is expanding? (Especially, hierarchical algorithms generally have run time $\Omega(n^2)$)

Finally, we describe the theoretical implication and future directions of our work.

5.3 Improve theoretical analysis

This work is a starting point in understanding and harnessing the impact of simple spectral algorithms in clustering problems. On the theoretical side, we have several important questions.

1. Can we have a more optimal analysis of k' -PC compression for $k' \neq k$?
2. What kind of correlation in the dataset can PCA handle, in terms of its compressibility impact? As a simple example, in our model if \hat{A} is rotated through an orthonormal operation, the inter-cluster and intra-cluster compression ratio due to PCA is unchanged, although the data is definitely not coordinate wise independent anymore.
3. What is a natural model that explains the underlying hierarchical clustering in datasets.

Acknowledgement

We are thankful to Shaddin Dughmi, Mi-Ying Huang, David Kempe and Sampad Mohanty for useful discussions. We specially thank Yingcong Li for the many important biological insights.

References

- [Abb18] Emmanuel Abbe. Community detection and stochastic block models: Recent developments. *Journal of Machine Learning Research*, 18(177):1–86, 2018.
- [CTP19] Joshua Cape, Minh Tang, and Carey E. Priebe. The two-to-infinity norm and singular subspace geometry with applications to high-dimensional statistics. *The Annals of Statistics*, 2019.
- [CZ18] T. Tony Cai and Anru Zhang. Rate-optimal perturbation bounds for singular subspaces with applications to high-dimensional statistics. *The Annals of Statistics*, 46(1):60 – 89, 2018.
- [DK70] Chandler Davis and W. M. Kahan. The rotation of eigenvectors by a perturbation. iii. *SIAM Journal on Numerical Analysis*, 7(1):1–46, 1970.
- [HHAN⁺21] Yuhan Hao, Stephanie Hao, Erica Andersen-Nissen, William M. Mauck III, Shiwei Zheng, Andrew Butler, Maddie J. Lee, Aaron J. Wilk, Charlotte Darby, Michael Zagar, Paul Hoffman, Marlon Stoeckius, Efthymia Papalexli, Eleni P. Mimitou, Jaison Jain, Avi Srivastava, Tim Stuart, Lamar B. Fleming, Bertrand Yeung, Angela J. Rogers, Juliana M. McElrath, Catherine A. Blish, Raphael Gottardo, Peter Smibert, and Rahul Satija. Integrated analysis of multi-modal single-cell data. *Cell*, 2021.
- [JW16] Jiashun Jin and Wanjie Wang. Influential features PCA for high dimensional clustering. *The Annals of Statistics*, 44(6):2323 – 2359, 2016.
- [KAH19] Vladimir Yu Kiselev, Tallulah S Andrews, and Martin Hemberg. Challenges in unsupervised clustering of single-cell rna-seq data. *Nature Reviews Genetics*, 20(5):273–282, 2019.

- [KMA⁺15] Allon M Klein, Linas Mazutis, Ilke Akartuna, Naren Tallapragada, Adrian Veres, Victor Li, Leonid Peshkin, David A Weitz, and Marc W Kirschner. Droplet barcoding for single-cell transcriptomics applied to embryonic stem cells. *Cell*, 161(5):1187–1201, 2015.
- [McS01] Frank McSherry. Spectral partitioning of random graphs. In *Proceedings 42nd IEEE Symposium on Foundations of Computer Science*, pages 529–537. IEEE, 2001.
- [TMN⁺16] Bosiljka Tasic, Vilas Menon, Thuc Nghi Nguyen, Tae Kyung Kim, Tim Jarsky, Zizhen Yao, Boaz Levi, Lucas T. Gray, Staci A. Sorensen, Tim Dolbeare, Darren Bertagnolli, Jeff Goldy, Nadiya Shapovalova, Sheana Parry, Changkyu Lee, Kimberly Smith, Amy Bernard, Linda Madisen, Susan M. Sunkin, Michael Hawrylycz, Christof Koch, and Hongkui Zeng. Adult mouse cortical cell taxonomy revealed by single cell transcriptomics. *Nature Neuroscience*, 19(2):335–346, 2016.
- [VKS17] K Kirschner V Kiselev and M Schaub. SC3: consensus clustering of single-cell RNA-seq data. *Nature Methods*, 14:483–486, 2017.
- [VU18] VAN VU. A simple svd algorithm for finding hidden partitions. *Combinatorics, Probability and Computing*, 27(1):124–140, 2018.
- [VWK⁺16] Trung Nghia Vu, Quin F. Wills, Krishna R. Kalari, Nifang Niu, Liewei Wang, Mattias Rantalainen, and Yudi Pawitan. Beta-Poisson model for single-cell RNA-seq data analyses. *Bioinformatics*, 32(14):2128–2135, 04 2016.